

Improved performance of Schottky diodes on pendeoepitaxial gallium nitride

T. Zheleva,^{1,a)} M. Derenge,¹ D. Ewing,¹ P. Shah,¹ K. Jones,¹ U. Lee,¹ and L. Robins²

¹Army Research Laboratory, SEDD, AMSRD-SE-RL, Adelphi, Maryland 20783, USA

²Materials Reliability Division, NIST, 325 Broadway, Boulder, Colorado 80305, USA

(Received 17 April 2008; accepted 18 August 2008; published online 5 September 2008)

We designed experiments to investigate the role of dislocation density on the performance of Schottky diodes fabricated on a GaN material grown conventionally and by pendeo-epitaxy. Devices of varying geometries were fabricated on low defect density GaN regions grown selectively via pendeo-epitaxy. In addition, corresponding devices were fabricated on the conventional GaN material with a high density of dislocations. Schottky diodes fabricated on pendeo-material showed nearly two orders of magnitude lower leakage current and displayed improved ideality factor, while diodes built on a conventional material displayed nonideal characteristics. © 2008 American Institute of Physics. [DOI: 10.1063/1.2978404]

Gallium nitride is a wide bandgap semiconductor having superior material characteristics for numerous electronic applications, compared to commonly used semiconductors such as Si and GaAs. The combined figure of merit for GaN as a material for high power, high frequency, high temperature applications is ~ 500 times higher than Si and over 60 times higher than GaAs.¹ However, long term device reliability is currently a critical issue that must be solved to enable the insertion of GaN devices and integrated circuits into systems. This is related to a number of failure mechanisms that arise from the degradation of material properties, associated with structural defects within the GaN layers and at the interfaces between GaN and other materials. One approach for the reduction of structural defect density in GaN material is via selective area epitaxy, a common name for both the lateral epitaxial overgrowth (LEO) and the pendeo-epitaxial (PE) growth techniques.^{2,3} The PE approach for growth of GaN utilizes the lateral epitaxial growth mechanism, enabling the GaN material to grow laterally from the side walls of etched GaN rectangular columns with two to four orders of magnitude lower density of dislocations than the conventional vertical growth techniques.³

GaN-based devices such as laser diodes, light emitting diodes, and p - n junctions showed significant improvement in operational characteristics such as lifetime, leakage current, and internal quantum efficiency, when the devices were fabricated on low defect density regions grown via selective area epitaxy.^{4,5} For example, an earlier study revealed that the reverse-bias leakage current in p - n junctions was reduced by three orders of magnitude on LEO GaN compared to the conventional GaN.⁴ A recent study on optimization of GaN-based high electron mobility transistors (HEMTs) by conventional metal-organic chemical vapor deposition (MOCVD) indicated that an increase in edge dislocation density is correlated with an increase in carrier trapping effects that, in turn, leads to stronger radio frequency dispersion.⁶ In another recent study, theoretical modeling suggested that dislocation-induced interface roughness in the channel of an AlGaIn/GaN HEMT structure was a primary cause of electron scattering, and hence reduced channel mobility.⁷ From the

modeling results, it was estimated that the use of pendeo-epitaxy will improve the low temperature and room temperature mobility of the two dimensional electron gas electrons in the HEMT by approximately 80% and 28%, respectively.

Our experiments were designed to investigate the role of the dislocation density on the performance of Schottky diodes fabricated on GaN material grown conventionally and by pendeo-epitaxy.⁸ A series of masks were designed to align electronic devices (e.g., Schottky diodes, Ohmic contacts, and gate source and drain for HEMTs) of various geometries with the low defect density regions of pendeo-epitaxially grown GaN, as shown in Fig. 1. The MOCVD growth parameters, such as growth temperature (1060–1120 °C), ammonia to trimethyl-gallium (V:III ratio of 1200 to 3600), chamber pressure 1.07×10^4 Pa (80 Torr) to 1.6×10^4 Pa (120 Torr), and mask geometry 2 μm or 3 μm stripe width, and 12 μm , 14 μm , or 20 μm stripe separation) were varied in order to optimize the lateral-to-vertical growth rate at a given pattern geometry. A wide range of material characterization techniques were used in order to establish the optimized growth and device processing parameters. The structural quality of the GaN material was characterized by

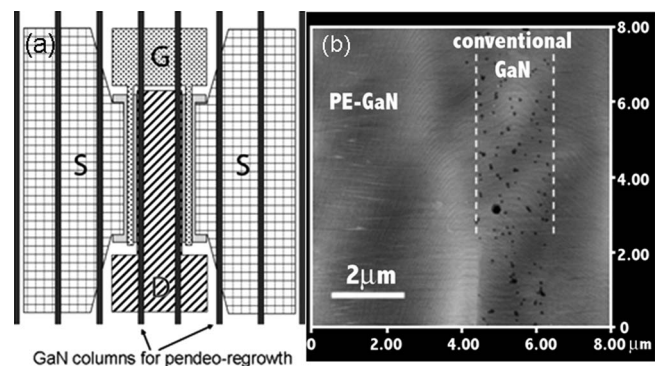


FIG. 1. (a) Schottky gates (g) of 2 μm length ($2 \times 100 \mu\text{m}^2$), aligned with the low defect density PE-GaN regions adjacent to the GaN columns of conventional GaN, shown in (b). The distances between the GaN columns are 14, 16, or 20 μm . (b) An AFM image of a GaN stripe revealing the difference in the dislocation density, $8.95 \times 10^8 \text{ cm}^{-2}$ for the column, conventional regions, and $2.8 \times 10^6 \text{ cm}^{-2}$ for the pendeo-wing regions (PE-GaN).

^{a)}Electronic mail: tzheleva@arl.army.mil.

scanning electron microscopy (SEM), atomic force microscopy (AFM), transmission electron microscopy, spectroscopic cathodoluminescence (CL), and etch pit density measurements. The distribution of dislocations throughout the material was determined by etching GaN with molten KOH at 450 °C for 5 min, to expose the areas with threading dislocations that have a higher etch rate than dislocation-free areas. Ohmic and Schottky contacts were fabricated, using standard lift-off photolithography on the two types of material in order to characterize the electrical properties of the low dislocation density pendeo-grown GaN material and the conventional (non-pendeo-) GaN material. The Ti (14 nm)/Al (220 nm) Ohmic contacts [source and drain regions in Fig. 1(a)] were annealed at 800 °C for 60 s prior to the Schottky contact metallization. The GaN was highly doped ($1 \times 10^{20} \text{ cm}^{-3}$) to ensure low resistance Ohmic contacts. The Ni (50 nm)/Au (150 nm) Schottky contacts were prepared via e-beam deposition. Device parameters, such as leakage current and ideality factor, were compared to Schottky diodes built on the pendeo- and the non-pendeo- (conventional) GaN regions and correlated with dislocation density.

The best GaN film quality and highest lateral-to-vertical growth rate ratio was achieved at growth temperatures of 1100–1120 °C, V:III ratio of 2600 and chamber pressure of 1.3×10^4 Pa (100 Torr).⁸ SEM images reveal that the PE “wing” areas of dimensions $(4\text{--}7 \text{ }\mu\text{m}) \times 100 \text{ }\mu\text{m}$, corresponding to lateral growth, are nearly free of dislocation-related etch pits. In comparison, the central regions of the stripes, corresponding to vertical growth, have a high density of etch pits. An AFM image of a GaN stripe, processed by the KOH etching technique to expose threading dislocations that propagate along or near the [0001] direction to the top surface, is shown in Fig. 1(b). The dislocations, revealed as etch pits, have densities of $(8.95 \pm 0.6) \times 10^8$ and $(2.8 \pm 3) \times 10^6 \text{ cm}^{-2}$ for the conventional (vertical growth) and the pendeo- (lateral growth) regions. Areas of PE GaN investigated by AFM as large as $5 \times 10 \text{ }\mu\text{m}^2$ were consistently observed to be free of dislocations. The root-mean-squared surface roughness of the non-pendeo- and the pendeo-GaN regions were $1.38 \pm 0.9 \text{ nm}$ and $0.3 \pm 0.08 \text{ nm}$, respectively. Thus, the dislocation density went through a drastic reduction of 320 times, while the surface roughness was reduced nearly five times.

Further characterization of the structural and optical properties of the pendeo- and non-pendeo-GaN material was performed via CL imaging and spectroscopy. A panchromatic plan view CL image that contains portions of five GaN stripes is shown in Fig. 2(a). The CL intensity is higher from the low defect density pendeo-GaN regions than from the non-pendeo-material in the center of each stripe. This difference is attributed to the presence of a higher density of non-radiative recombination centers in the non-pendeo-material, associated with impurities and point defects clustered around the dislocation cores.⁹ Local areas of lower CL intensity (dark contrast), with a highly nonuniform spatial distribution, are also observed near the outer edges of the pendeo-grown regions adjacent to the gaps between the GaN stripes. These localized “dark contrast” areas are attributed to the extended defects, mostly threading dislocations, that propagate initially vertically from the center of the stripes and then laterally to the outer edges of the stripes (Note that the CL inten-

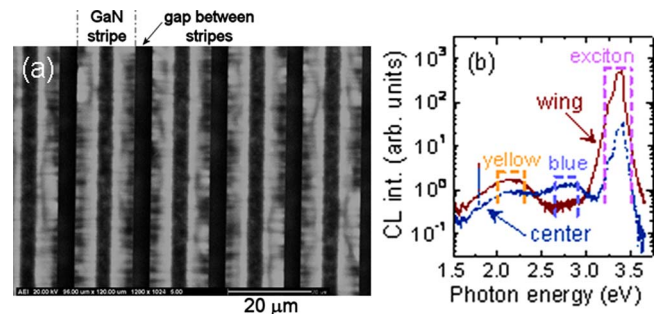


FIG. 2. (Color online) (a) CL image in panchromatic mode showing portions of five adjacent GaN stripes grown via pendeo-epitaxy. (b) CL spectra acquired from the center, column (conventional) and wing (pendeo-) areas of a stripe, reveal nearly 15 times increase in the CL intensity of the NBE excitonic peak from the pendeo-regions, due to the reduced number of non-radiative traps.

sity is also very low from the gaps between the GaN stripes). CL spectra in the 1.5–3.7 eV range were acquired from the center and wing regions, as shown in Fig. 2(b). There is over one order of magnitude increase in the photoluminescence intensity of the near band edge (NBE) or excitonic peak (in the 3.2–3.5 eV range), from the pendeo-GaN region, as compared to the conventional region. Interestingly, the pendeo-material shows a stronger “yellow” band (2.0–2.3 eV), by about a factor of 2, than the non-pendeo-material. On the other hand, the non-pendeo-material shows a relatively strong “blue” band (2.65–2.9 eV), while the pendeo-material does not show a distinct peak in the blue region. The blue and yellow luminescence bands in GaN are attributed to impurities or (impurity, point defect) complexes; several models have been proposed for the relevant luminescence centers. The yellow luminescence band has been ascribed to deep donor kaceptor recombination involving C and O impurities,⁹ or to complexes, gallium vacancy and C or O impurity, acting as deep acceptors.¹⁰ The blue band has been ascribed to deep donor–acceptor recombination, involving C impurities,¹¹ or to Zn deep acceptors.¹⁰ The observation that the intensity of the yellow band is reduced by a factor of 2 in the high dislocation density conventional GaN regions (as compared to the pendeo-grown regions) suggests that the yellow band is quenched by the same nonradiative recombination centers, associated with dislocations, that give rise to the quenching of the exciton band in the non-pendeo-regions. The observation that a distinct blue band occurs only in non-pendeo-regions suggests that the blue luminescence centers (impurities and point defects) occur near the dislocation cores.

Schottky Ni (50 nm)/Au (150 nm) contacts aligned with the low defect density pendeo-GaN stripes are shown in Fig. 1(a). The current-voltage (I - V) characteristics of the Schottky diodes aligned with the low defect density pendeo-GaN stripes fabricated on the pendeo- and non-pendeo-GaN regions were measured between -10 and 5 V , as shown in Fig. 3.¹² These measurements were performed for ten individual diodes fabricated on each pendeo- and non-pendeo-regions. The ideality factor n describes how closely the Schottky diode follows the thermionic emission theory. A perfectly ideal diode has $n=1.0$. Schottky contacts with closer to 1 ideality factors indicate an improved metal-semiconductor interface, while higher ideality factors indicate current transport mechanisms other than thermionic

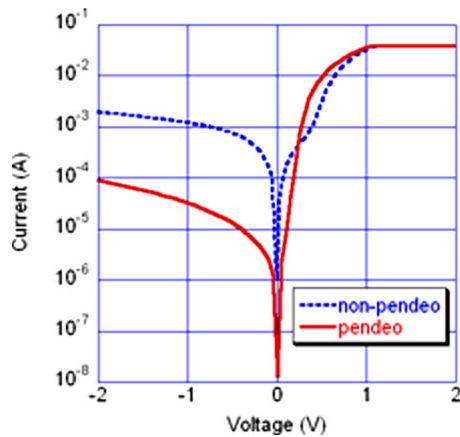


FIG. 3. (Color online) Current-voltage (I - V) characteristics of Schottky diodes to PE-GaN (solid line) and conventional, non-pendeo-GaN (dashed), displaying nonideal characteristics.

emission. Schottky diodes fabricated on non-pendeo-material displayed nonideal characteristics with an average ideality factor $n = 1.73 \pm 0.35$. Conversely, Schottky diodes on PE material displayed significantly closer to ideal characteristics under forward bias with an average ideality factor $n = 1.32 \pm 0.04$. While the Schottky diodes on the peudeo-GaN material is displayed close to ideal linear behavior, the Schottky diodes on the non-pendeo-stripes all displayed a characteristic “kink” at low forward voltage that is typical of two barrier heights acting in parallel.¹³ These phenomena occur when “patches” of inhomogeneous Schottky barrier height materials are present at the metal-semiconductor interface. In addition, at a -2 V reverse bias, the average leakage current was measured to be $(6.7 \pm 2.8) \times 10^{-5}$ and $(2.1 \pm 6.8) \times 10^{-4}$ A for the peudeo- and non-pendeo-material, respectively. The large standard deviation of the leakage current for each type of material (which represents a statistical distribution of measurements in many Schottky diodes) can be explained by assuming that some diodes are in close proximity to an extended defect such as a threading dislocation core, which gives rise to a higher than average leakage current. This “defect proximity effect” is more likely to occur for devices fabricated in a non-pendeo-material than a peudeo-material because of the much higher dislocation density. Hence, the standard deviation of the leakage current is higher in the non-pendeo- than peudeo-material. These variations can be over an order of magnitude from the lowest value to the highest value. The current densities for the peudeo- versus conventional Schottky diodes measured at -2 V were 54.5 versus 117 A/cm², respectively. Due to the geometry of our Schottky contacts and the large doping concentration, our data are not strictly comparable on a purely

number basis to the existing data in literature for circular Schottky contacts, for example, Ref. 14. Our Schottky to Ohmic contact spacing is 2 μm compared to the larger spacing of 25 μm in Ref. 14. This and the fact that our contacts are parallel with corner points compared to the concentric circular contacts in Ref. 14 will lead to higher fields in the GaN layer and, thus, increased leakage current density. In addition, our GaN material is highly doped, which would also contribute to the large leakage current via larger contribution of the tunneling of electrons through the barrier. Overall, the diodes on the PE material show more uniformity in terms of ideality and leakage current, due to the lower defect density material. The reduction of the leakage current density by a factor of 2 is another indication of the improved electrical properties of the PE material.

In summary, optimization of the MOCVD growth parameters enabled us to produce low defect density PE GaN material within a large area $[(4-7) \times 100 \mu\text{m}^2]$. Schottky diodes fabricated on the PE-GaN showed about an order and a half magnitude reduction in leakage current and approximately 25% improvement in ideality factor, as compared to diodes of similar structure fabricated on non-pendeo-material. Improvement of the metal-semiconductor contacts is expected to lead to further enhancement of the performance of PE based devices.

- ¹T. P. Chow and R. Tyagi, *IEEE Trans. Electron Devices* **41**, 1481 (1994).
- ²T. S. Zheleva, O.-H. Nam, W. M. Ashmawi, J. D. Griffin, and R. F. Davis, *J. Cryst. Growth* **222**, 706 (2001).
- ³T. S. Zheleva, S. Smith, D. Thomson, K. Linthicum, P. Rajagopal, and R. F. Davis, *J. Electron. Mater.* **28**, L5 (1999), and the references therein.
- ⁴P. Kozodoy, J. P. Ibbetson, H. Marchand, P. T. Fini, S. Keller, J. S. Speck, S. P. DenBaars, and U. K. Mishra, *Appl. Phys. Lett.* **73**, 975 (1998).
- ⁵K. Nishizuka, M. Funato, Y. Kawakami, S. Fujita, Y. Narukawa, and T. Mukai, *Appl. Phys. Lett.* **85**, 3122 (2004).
- ⁶D. S. Green, S. R. Gibb, B. Hoisse, R. Veturly, D. E. Grider, and J. A. Smart, *J. Cryst. Growth* **272**, 285 (2004).
- ⁷K. A. Bulashevich, S. Y. Karpov, Y. N. Makarov, T. S. Zheleva, P. B. Shah, M. A. Derenge, and K. A. Jones, *Phys. Status Solidi C* **5**, 1980 (2008).
- ⁸T. S. Zheleva, M. A. Derenge, K. A. Jones, P. B. Shah, D. J. Ewing, J. Molstad, U. Lee, M. H. Ervin, and D. N. Stepp, Proceedings of the 25th US Army Science Conference, Orlando, FL, 27–30 November 2006 (unpublished).
- ⁹D. M. Hofmann, D. Kovalev, G. Steude, B. K. Meyer, A. Hoffmann, L. Eckey, R. Heitz, and T. Detchprom, *Phys. Rev. B* **52**, 16702 (1995).
- ¹⁰M. A. Reschikov and H. Morkoc, *Physica B (Amsterdam)* **376**, 428 (2006).
- ¹¹R. Armitage, Q. Yang, and E. R. Weber, *J. Appl. Phys.* **97**, 073524 (2005).
- ¹²D. J. Ewing, M. A. Derenge, P. B. Shah, U. Lee, T. S. Zheleva, and K. A. Jones, *J. Vac. Sci. Technol. B* **26**, 1368 (2008).
- ¹³R. T. Tung, *Phys. Rev. B* **45**, 13509 (1992).
- ¹⁴J. Spradlin, S. Dogan, D. Huang, L. He, D. Johnstone, H. Morkoc, and R. J. Molnar, *Appl. Phys. Lett.* **82**, 3556 (2003).